



NRC Publications Archive Archives des publications du CNRC

Description of a four degrees of freedom, V/STOL aircraft, airborne simulator

Daw, D. F.; Lum, K.; McGregor, D. M.

For the publisher's version, please access the DOI link below./ Pour consulter la version de l'éditeur, utilisez le lien DOI ci-dessous.

Publisher's version / Version de l'éditeur:

<https://doi.org/10.4224/21272068>

National Research Council of Canada Aeronautical Report, 1968-02

NRC Publications Record / Notice d'Archives des publications de CNRC:

<https://nrc-publications.canada.ca/eng/view/object/?id=5989cb18-a63d-44b4-b479-765790d80bcc>

<https://publications-cnrc.canada.ca/fra/voir/objet/?id=5989cb18-a63d-44b4-b479-765790d80bcc>

Access and use of this website and the material on it are subject to the Terms and Conditions set forth at

<https://nrc-publications.canada.ca/eng/copyright>

READ THESE TERMS AND CONDITIONS CAREFULLY BEFORE USING THIS WEBSITE.

L'accès à ce site Web et l'utilisation de son contenu sont assujettis aux conditions présentées dans le site

<https://publications-cnrc.canada.ca/fra/droits>

LISEZ CES CONDITIONS ATTENTIVEMENT AVANT D'UTILISER CE SITE WEB.

Questions? Contact the NRC Publications Archive team at

PublicationsArchive-ArchivesPublications@nrc-cnrc.gc.ca. If you wish to email the authors directly, please see the first page of the publication for their contact information.

Vous avez des questions? Nous pouvons vous aider. Pour communiquer directement avec un auteur, consultez la première page de la revue dans laquelle son article a été publié afin de trouver ses coordonnées. Si vous n'arrivez pas à les repérer, communiquez avec nous à PublicationsArchive-ArchivesPublications@nrc-cnrc.gc.ca.



National Research
Council Canada

Conseil national de
recherches Canada

Canada

NATIONAL RESEARCH COUNCIL OF CANADA

AERONAUTICAL REPORT
LR-499

DESCRIPTION OF A FOUR DEGREES OF FREEDOM,
V/STOL AIRCRAFT, AIRBORNE SIMULATOR

D. F. DAW, K. LUM AND D. M. MCGREGOR
NATIONAL AERONAUTICAL ESTABLISHMENT

OTTAWA
FEBRUARY 1968

NRC NO. 10182

TABLE OF CONTENTS

| | Page |
|--|-------|
| SUMMARY | (iii) |
| TABLE | (iv) |
| ILLUSTRATIONS | (iv) |
| SYMBOLS | (v) |
| APPENDICES | (vi) |
| 1.0 INTRODUCTION | 1 |
| 2.0 GENERAL DESCRIPTION OF THE SIMULATOR | 1 |
| 3.0 DESCRIPTION OF EQUIPMENT | 3 |
| 3.1 Analogue Computer | 3 |
| 3.2 Equipment Associated with the Computer | 4 |
| 3.3 Autopilot | 5 |
| 3.3.1 Lead or Pre-emphasis | 5 |
| 3.3.2 Control Loop Compensation | 5 |
| 3.3.3 Positional Servo Actuators | 6 |
| 3.3.4 Feedback Sensors | 7 |
| 3.3.5 Filtering | 7 |
| 3.4 Tape Recorder | 7 |
| 3.5 Synthetic Instrument Landing System (I.L.S.) | 7 |
| 4.0 CONCLUDING REMARKS | 7 |
| 5.0 REFERENCES | 8 |

TABLE

| Table | Page |
|---|------|
| 1 Undamped Natural Frequency for Four Control Loops | 13 |

ILLUSTRATIONS

| Figure | Page |
|---|------|
| 1 Four Degrees of Freedom V/STOL Airborne Simulator | 15 |
| 2 "Model-Controlled" Simulation Method | 16 |

ILLUSTRATIONS (Cont'd)

| Figure | Page |
|---|------|
| 3 View of the Simulator Cockpit from the Right Side | 17 |
| 4 The Analogue Computer Used for the Model | 18 |
| 5 View of the Simulator Cockpit from the Left Side | 19 |
| 6 Orange Sub-Cockpit Installation for Simulated Instrument Flying | 20 |
| 7 Power Spectrum of Simulated Atmospheric Turbulence | 21 |
| 8 Autopilot Schematic | 22 |
| 9a Frequency Response for Yaw Control Loop | 23 |
| 9b Frequency Response for Pitch Control Loop | 24 |
| 9c Frequency Response for Roll Control Loop | 25 |
| 9d Frequency Response for Heave Control Loop | 26 |
| 10 Analogue Computer Study on the Effect of Lead Network on Helicopter Transient Response | 27 |
| 11 Autopilot Actuator System | 28 |
| 12 Synthetic Instrument Landing System | 29 |
| 13 Illustrative Computer Wiring Diagram for the Directional Equation of Motion | 30 |

SYMBOLS

| Symbol | Definition |
|--------|--|
| C | Yawing moment of inertia, slug ft ² |
| E | Product of inertia, slug ft ² |
| F.M. | Frequency modulated |
| Hz | Cycles per sec |
| ips | Inches per sec |
| K | Gain in autopilot compensation and Gain in turbulence expression |

SYMBOLS (Cont'd)

| Symbol | Definition |
|---------------|--|
| L | Scale length of turbulence, ft |
| N | Yawing angular acceleration per unit subscript, $\text{rad/sec}^2/\text{unit subscript}$ |
| p | Angular rate of roll, rad/sec |
| r | Angular rate of yaw, rad/sec |
| S | Laplace operator |
| t | Time, sec |
| T | Time constant in autopilot compensation |
| V | Flight velocity, ft/sec |
| α | Angle of attack, rad |
| β | Angle of sideslip, rad |
| δ_a | Pilot's roll control deflection, in |
| δ_r | Pilot's yaw control deflection, in |
| $\ddot{\psi}$ | Angular acceleration in yaw, rad/sec^2 |
| $\ddot{\phi}$ | Angular acceleration in roll, rad/sec^2 |
| ω | Frequency, rad/sec |
| ω_N | Undamped natural frequency, rad/sec |

Subscripts

H Helicopter

Other subscripts are defined above.

APPENDICES

| App. | Page |
|--------------------|------|
| A Appendix A | 31 |

DESCRIPTION OF A FOUR DEGREES OF FREEDOM,
V/STOL AIRCRAFT, AIRBORNE SIMULATOR

1.0 INTRODUCTION

It is widely recognized that the development of vertical and short take-off and landing aircraft is still in its relative infancy. There remain many unknowns in establishing optimum or, in fact, acceptable handling qualities, the most suitable modes of flight operations, particularly under instrument conditions, satisfactory flight instruments to allow the pilot to utilize the aircraft's potentials fully, meaningful design criteria, and other facets of their design and use. Current helicopter and V/STOL aircraft specifications (Ref. 1 and 2) were formulated largely from experience with helicopters that, in general, were very different from the present and the proposed generation of V/STOL aircraft.

Clearly, a need exists for a versatile airborne simulator capable of reproducing and simulating, with high fidelity, a wide range of flying characteristics applicable to this new breed of aircraft. Such a research tool makes it possible to investigate the above problems in a systematic and controlled manner in the proper airborne environment.

The first attempt, by the National Aeronautical Establishment, to fill this requirement resulted in the development of the variable stability helicopter described in Reference 3. The flight characteristics of this simulator could be altered significantly about its three rotational degrees of freedom by use of the model-controlled method of simulation, and enabled a variety of handling qualities investigations to be successfully completed (e.g. Ref. 4 and 5).

With the experience of building and operating the three degrees of freedom simulator, the development of a vastly improved variable stability helicopter was undertaken incorporating the capability to alter its characteristics in the vertical, or heave channel, as well as the three rotational modes of motion. An electro-hydraulic autopilot and an increased computing capacity have greatly enhanced its usefulness and have yielded a reliable and yet flexible simulator. This is demonstrated in the three programs reported in References 6, 7, and 8 - one of a general research nature and the other two simulations of particular aircraft.

This Report describes the equipment installed in the helicopter to achieve its variable stability capability and indicates how it is used to simulate various flight characteristics.

The Appendix contains an illustration of how the equations of motion are programmed for use with the simulator.

2.0 GENERAL DESCRIPTION OF THE SIMULATOR

The basic vehicle used for this airborne simulator is a light, single rotor helicopter, a Bell 47G-3B1 (Fig. 1) with a maximum gross weight of 2950 pounds and powered by a turbo-supercharged engine. This latter feature is useful in maintaining

the full engine power in summer months during the prolonged hovering and low speed flight necessary to evaluate certain V/STOL aircraft characteristics.

It will be noted from Figure 1 that the stabilizer bar, one fuel tank, and the battery have been removed to lighten the aircraft, allowing the installation of more computing components and project equipment. Even with the fuel capacity reduced in this way, the available testing time is still in excess of $1\frac{1}{4}$ hours.

Since the simulator system ultimately relies on the basic helicopter controls to produce the desired motions, the maximum accelerations (control powers) employed in simulations are limited to those attainable by the helicopter. These are quite high, however, when compared with existing V/STOL aircraft in the low speed flight regime, and have been measured to be 2.4 rad/sec^2 in yaw, 1.2 rad/sec^2 in pitch, 2.2 rad/sec^2 in roll, and 8 ft/sec^2 in heave.

Two pilots occupy the simulator during all flight tests, with the one on the left side acting as safety pilot as well as program manager and the one on the right flying the aircraft through the "fly-by-wire" system while assessing the handling qualities being simulated. A screen is installed between the two cockpits to prevent the evaluation pilot from seeing the safety pilot's control movements, which in some cases are entirely different from his own and, hence, are quite disconcerting if in his field of view.

The simulation method used is the "model-controlled" method (Ref. 9), which was demonstrated by the original simulator to achieve accurate and predictable flight characteristics without a detailed knowledge of the stability and control characteristics of the basic vehicle. With this approach to simulation (Fig. 2), movements of the evaluation pilot's electric flying controls (Fig. 3) supply signals proportional to control deflections to the analogue computer. The computer (Fig. 4) is "patched" for the characteristics of the equations of motion to be simulated and yields signals that are properly scaled to represent the yaw, pitch, and roll angular rates, and the normal acceleration of the simulated vehicle. These calculated motions are compared with those of the helicopter, as sensed by angular rate gyros and normal accelerometers, and the autopilot, operating in a closed-loop fashion, forces the helicopter to follow the motions prescribed by the computer. Other inputs to the equations of motion such as synthetic turbulence, simulated steady winds, and angles of attack and sideslip as measured by vanes, can be utilized to produce realistic simulations of very high fidelity. This simulation method has the advantages of preventing the trim changes occurring on the test aircraft from being felt by the evaluation pilot and resisting disturbances in the controlled degrees of freedom that are due to external turbulence.

All four of the autopilot actuators are connected in parallel with the safety pilot's controls. In the main rotor collective, and both the longitudinal and lateral cyclic systems they are located before the irreversible hydraulic boost cylinders normally part of the basic helicopter. The inherent directional control forces are very light; consequently, the yaw autopilot actuator was connected directly to the tail rotor collective pitch system in parallel with the safety pilot's pedals. Since the autopilot has 100 percent authority, this method of attachment was necessary to keep the safety pilot informed of the true control positions and enable him to assume positive control at any time.

The analogue computer and autopilot are controlled, trimmed, programmed

and monitored by the switches, gain-setting potentiometers, function switches, and meter, mounted on the console situated between the pilots in the cockpit and shown in Figure 5.

The evaluation pilot's control levers can assume any form providing electrical signals proportional to their deflections can be obtained. "Power lever" and "collective" height controls have been utilized as well as a conventional control column and a wheel for pitch and roll control. Spring feel with viscous damping and adjustable friction have been used with the roll, pitch, and yaw controls, while adjustable friction only is provided for the height control. Both "beep" and "push-to-release" trimmers are available for the control column. A more flexible electro-hydraulic feel system is being designed for installation in the near future.

Two pods are mounted externally, as shown in Figure 1, with the one on the port side housing the main portion of the analogue computer (Fig. 4) while that on the starboard side accommodates various power supplies, a 14-channel tape recorder, plus miscellaneous electronic equipment including the circuitry associated with the engine speed governor.

The engine speed, and consequently the rotor speed, are governed by an electro-hydraulic control system allowing duplication of conditions existing in modern V/STOL aircraft equipped with free turbine engines. The evaluation pilot has been provided with a "beep" trimmer for this system, which is normally installed on his power lever or collective control.

An instrument flight panel containing the six basic flight instruments, together with two engine instruments and the instrument landing system cross-pointer driven by the ground installation described in Section 3.5, is situated in front of the evaluation pilot (Fig. 3). These instruments can be rearranged, replaced, or other instruments added, as was done for the research of Reference 8. During instrument flight evaluation tasks, an orange sub-cockpit is installed on the right side (Fig. 6) and the pilot dons blue goggles, this combination preventing him from viewing the external world while he refers only to his instruments for flight information.

3.0 DESCRIPTION OF EQUIPMENT

3.1 Analogue Computer

The heart of this simulation method is, of course, the computer used to build up the model of the aircraft to be simulated. Standard electrical analogue plug-in components, which are directly interchangeable with laboratory units, have been mounted in the fibreglass pods for this installation (Fig. 4). The basic computer consists of:

- (i) 76 operational amplifiers (16 of which are used in the autopilot);
- (ii) 30 integrating networks or non-linear elements such as diode function generators, multipliers, etc;
- (iii) 50 attenuators or gain-setting potentiometers (20 of which are situated on the centre console in the cockpit to enable the safety pilot to change characteristics without unstrapping);

- (iv) 12 function switches, also available to the safety pilot to preset changes of conditions such as stability augmentation failures (Ref. 7 and 8);
- (v) 2 relays with 4 double throw positions, which can be actuated by a switch on the safety pilot's collective handle to effect various changes in a stepwise fashion;
- (vi) a transport time delay unit with a capability of inserting delays from 0.1 sec to 160 sec;
- (vii) 2 "track-and-hold" circuits that are used to eliminate transients as the vanes are switched in and out of the model when the aircraft departs and approaches hovering flight (see Para 3.2 (i));
- (viii) 60 balancing controls located in the cockpit, one for each amplifier used in the model;
- (ix) 60 overload lights situated in front of the safety pilot that indicate when the amplifiers exceed their limits of linear operation;
- (x) an overload horn that sounds in the safety pilot's left ear when any amplifier reaches its limit;
- (xi) patching points to connect the computing components together and to introduce the signals from the various transducers, described in the next Section, into the electrical analogue;
- (xii) power supplies that have been especially designed and packaged to minimize both weight and space.

All these components can be "patched" together to simulate quite complex fixed-point equations of motion in the four controlled degrees of freedom.

3.2 Equipment Associated with the Computer

A variety of transducers and simulating elements have been installed in the aircraft for use in the equations of motion. These include:

- (i) Angle of attack and angle of sideslip vanes that are used in forward flight above 25 knots to drive potentiometers yielding signals proportional to these parameters. These vanes are normally switched into the simulation during acceleration from the hover (around 30 knots indicated airspeed) and switched out as the helicopter decelerates through 20 - 25 knots on the approach to landing. Appropriate "track-and-hold" circuits prevent transients as the changes are made.
- (ii) A directional gyro that yields signals proportional to (a) the heading of the aircraft, (b) the change of angle from the heading at which the system is engaged, and (c) the sine and cosine of this change of heading, which can be used to simulate the effects of a wind on the longitudinal and lateral velocities as the helicopter is turned in the hover.
- (iii) A vertical gyro that yields signals proportional to the roll and pitch angles and has proven useful in simulating various attitude hold features of stability augmentation systems.

(iv) Two lateral accelerometers situated with respect to the centre of gravity to minimize the effects of yawing and rolling angular accelerations. These accelerometers were used in the research of Reference 8 as one source of directional stabilization.

(v) Three statistically independent synthetic turbulence generators that may be programmed at any gust intensity level to give realistic flight disturbances. These devices contain Geiger tubes and radioactive elements to provide sources of random pulses (Ref. 10), and their outputs can be shaped by active filters to yield power spectra approximating those of atmospheric turbulence. A typical shape used is shown in Figure 7.

3.3 Autopilot

The desired helicopter responses are calculated by the analogue computer and, as indicated by the diagram of Figure 2, are compared with the actual helicopter motions measured by angular rate gyros and normal accelerometers mounted on the aircraft. To make the autopilot control loops operate in the optimum fashion, each consists of a "lead" term (or pre-emphasis), a compensation network, a hydraulic positional servo actuator, the basic aircraft, a feedback sensor, and a filter network (Fig. 8).

Various safety devices are built into the system to allow the safety pilot to assume positive control of the aircraft should a dangerous situation arise. One of these is a circuit that automatically disengages the autopilot following a failure of any one of six critical voltages in the system, and simultaneously sounds an audio alarm in the safety pilot's earphone.

The frequency response for each autopilot control loop, shown in Figure 9, was obtained by determining the transfer function for each system component. It was not practical to determine the actual frequency response of each control loop experimentally since this would have required forcing the aircraft at frequencies that would excite structural modes, causing damage to the helicopter. Hence, only the undamped natural frequencies were obtained by increasing the loop gains until sustained oscillations occurred. In most cases the experimental results shown in Table I are in fair agreement with those determined from transfer function analysis.

3.3.1 Lead or Pre-emphasis

In order to improve the response of the simulator, a "lead" compensation network has been placed between the model and the hydraulic servo in each channel (Fig. 8). These circuits attempt to eliminate the lags due to the basic helicopter by pre-emphasizing the model command signal, and have succeeded in enhancing the system performance as indicated in the frequency and time domains in Figures 9 and 10. The insertion of these lead terms does not affect the closed loop system stability, sensitivity to external disturbances, etc., but only pre-emphasizes the model outputs to the autopilot.

3.3.2 Control Loop Compensation

Good model-following characteristics of the airborne simulator require the control system to have high closed loop gain and wide bandwidth relative to the bandwidth of the signal from the model. High gain is essential for fast transient response,

but the usable gain is limited by system overshoot and stability.

Compensation circuits of the form $\frac{K(1+TS)}{S}$ have been applied to the angular rate control loops to make them Type 1 systems. This ensures infinite open loop gains for dc signals without significantly increasing the phase lags at higher frequencies that would tend to reduce the undamped natural frequencies.

For the heave control loop the compensation is of the lag-lead-lag form, to cancel out the zero at $S = 0$ term in the transfer function describing the helicopter vertical acceleration to collective control inputs.

It was found necessary to incorporate a gain change circuit in the pitch control loop because of the increasing control sensitivity of the basic helicopter with increasing speed resulting from the aerodynamic effect of the controllable elevator. In order to maintain an optimum closed-loop gain throughout, the autopilot gain is high at low speed and vice versa, with the alteration being made smoothly by a light-sensitive resistance illuminated by a modulated lamp actuated by a speed-sensitive, spring-loaded vane at the front of the helicopter. This gain change occurs at approximately 45 knots. The other three control loops remain invariant with flight condition.

3.3.3. Positional Servo Actuators

Each autopilot channel is connected to the appropriate helicopter control through a hydraulic actuator (Fig. 11). To keep the frequency response of the overall system high these actuators have been made positional controls, with the position feedback being obtained from film potentiometers mounted on the actuator body.

Since it is necessary to engage the autopilot in a variety of flight conditions from still air hover to high speed flight, track-and-hold circuits are installed in each feedback path, which keeps the position signals zero until the autopilot is engaged. Actuator changes from their initial positions are then measured and used in this control loop. These circuits are disengaged when the safety pilot actuates a spring-loaded button on the top of the control column, altering the actuator to an integrating type, thus enabling him to accurately trim the positional loop before leaving the ground. While this button is engaged the integrating capacitors in the compensation networks are short-circuited, preventing any signals from the feedback transducers from affecting the actuator trim.

High response electro-hydraulic valves control the flow to the actuators, while both an engine-driven pump and a pump driven by an electric motor during ground testing are available to supply the 250 psi hydraulic pressure for system operation.

The safety pilot can override the system by overpowering the autopilot actuators with forces of 17 lb in the longitudinal cyclic, 14 lb in the lateral cyclic, 25 lb on the tail rotor pedals, and 13 lb on the main rotor collective. Check valves (Fig. 11) have been incorporated around each actuator to make it possible for the pilot to move the controls by exerting forces just slightly higher than those above, even if the electro-hydraulic valve fails in the fully closed position. The entire autopilot (and engine speed governor) can be disengaged by either pilot through buttons located on their control columns, which allows hydraulic fluid to be pumped freely from

one side of the actuator to the other through the "by-pass" valve shown in Figure 11.

3.3.4 Feedback Sensors

The angular velocity of the simulator in each rotational degree of freedom is sensed by a high natural frequency (30 Hz) rate gyro with a linear range of ± 60 deg/sec. The three gyros that provide the electrical signals for comparison with the angular rates calculated in the model are mounted on a machined block that has been carefully aligned with the aircraft axes.

Two linear accelerometers, mounted with respect to the centre of gravity to eliminate signals due to pitching and rolling accelerations, provide the feedback signal to be compared with the calculated normal accelerations from the model. These devices are subminiature "force-balance" servo systems that have natural frequencies of 100 Hz.

3.3.5 Filtering

Since the transducers in the autopilot feedback loops respond to motions of the simulator, they also are affected by the relatively high vibration level inherent in the helicopter caused by rotating components such as the main and tail rotors and the engine. To prevent this noise from limiting the useable gain in each autopilot closed loop, the signal from each transducer is filtered by a network designed to eliminate the bothersome signals and yet minimize the phase lag at low frequencies. The frequency response information contained in Figure 9 was obtained including the filters.

3.4 Tape Recorder

A 14-channel magnetic tape recorder is installed in the starboard pod and is currently set up to record 13 channels of F.M. data and one channel of audio at 1-7/8 ips. Up to 13 parameters in the equations of motion or the responses of the simulator may be recorded while the audio channel is used to record the pilot's comments. Three calibration pulses on each F.M. channel are automatically recorded after the pilot selects the recorder on.

3.5 Synthetic Instrument Landing System (I.L.S.)

Using the orange-blue system described previously, this vehicle can be used to simulate instrument flying conditions. To provide a flexible, meaningful, instrument task, a synthetic instrument landing system has been developed that allows selection of any localizer angle and any glide path angle up to approximately 30 deg. In addition, the localizer and glide path beam sensitivities can be adjusted over a wide range.

The system, shown pictorially in Figure 12, involves an operator on the ground optically tracking the helicopter in both azimuth and elevation, while the errors from the desired flight path are transmitted continuously to the helicopter and displayed to the evaluation pilot on a cross-pointer type of instrument.

4.0 CONCLUDING REMARKS

The original three degrees of freedom simulator employed at this Establishment

proved to be a valuable airborne research tool. The results from the several programs completed to date, utilizing the greatly improved capabilities of the four degrees of freedom simulator described in this Report, show that it provides an even more versatile means of conducting experiments relating to the stability and control of VTOL and STOL aircraft.

5.0 REFERENCES

1. U.S. Department of Defense Military Specification, Helicopter Flying and Ground Handling Qualities: General Requirements. MIL-H-8501A, 7 Sept. 1961.
2. Recommendations for V/STOL Handling Qualities. AGARD Report 408, Advisory Group for Aeronautical Research and Development (NATO), October 1962.
3. Daw, D.
McGregor, D.M. Development of a Model-Controlled V/STOL Airborne Simulator. NRC, NAE Aero. Report LR-352, National Research Council of Canada, August 1962.
4. McGregor, D.M. An Investigation of the Effects of Lateral-Directional Control Cross-Coupling on Flying Qualities using a V/STOL Airborne Simulator. NRC, NAE Aero. Report LR-390, National Research Council of Canada, December 1963.
5. Smith, R.E. A Comparison of V/STOL Aircraft Directional Handling Qualities Criteria for Visual and Instrument Flight using an Airborne Simulator. NRC, NAE Aero. Report LR-465, National Research Council of Canada. Sept. 1966.
6. McGregor, D.M. The Influence of Aircraft Size on Control Power and Control Sensitivity Requirements. A Comparison of Results from Two Variable Stability Helicopters. NRC, NAE Aero. Report LR-459, National Research Council of Canada, July 1966.
7. McGregor, D.M. Simulation of the Canadair CL-84 Tilt-Wing Aircraft using an Airborne V/STOL Simulator. NRC, NAE Aero. Report LR-435, National Research Council of Canada, July 1965.
8. McGregor, D.M. A Flight Investigation of Various Stability Augmentation Systems for a Jet-Lift V/STOL Aircraft (Hawker Siddeley P1127) using an Airborne Simulator. (NRC, NAE Aero. Report LR-500, National Research Council of Canada, Feb. 1968.

9. Gould, D.G.

The Model Controlled Method for the Development of Variable Stability Aircraft. NRC, NAE Aero. Report LR-345, National Research Council of Canada, June 1962.

10.

Random Noise Generator for Simulation Studies. Goodyear Aircraft Corp., Akron, Ohio, Report GER-6436, December 1954.

APPENDIX A

As an example of how the model is programmed and scaled for use in this model-controlled method, consider how a typical directional equation of motion is simulated. Let the yawing acceleration be

$$\ddot{\psi} = N_{\delta_r} \cdot \delta_r + N_{\delta_a} \cdot \delta_a + N_r \cdot r + N_p \cdot p + N_\beta \cdot \beta + \frac{E}{C} \dot{\phi}$$

where each of the terms is defined in the list of symbols.

The stability derivatives have dimensions of rad/sec^2 per unit variable (e.g. N_{δ_r} , $\frac{\text{rad/sec}^2}{\text{inch of rudder}}$) obtained by dividing the yawing moment per unit variable by the yawing moment of inertia of the simulated aircraft.

Each variable is scaled in the normal analogue computer fashion to utilize as much of the linear range of the amplifiers as possible, allowing for the anticipated maximum variations. The only voltage scaling that cannot be altered is at the final step, where the model is compared with the helicopter angular rate since the helicopter scaling from the rate gyro to the amplifier used as the comparator in the autopilot is determined by the autopilot closed loop gain.

Using the optimized scaling terms as defined in the list of symbols, and calculating the yaw rate instead of the acceleration, gives the following scaled equation

$$K_r \dot{\psi} = \left(\frac{K_r}{K_{\delta_r}} N_{\delta_r} \right) \int_0^t K_{\delta_r} \cdot \delta_r dt + \left(\frac{K_r}{K_{\delta_a}} N_{\delta_a} \right) \int_0^t K_{\delta_a} \cdot \delta_a dt + (N_r) \int_0^t K_r \cdot r dt \\ + \left(\frac{K_r}{K_p} N_p \right) \int_0^t K_p \cdot p dt + \left(\frac{K_r}{K_\beta} N_\beta \right) \int_0^t K_\beta \cdot \beta dt + \left(\frac{K_r}{K_p} \frac{E}{C} \right) K_p \cdot p$$

where the terms in the brackets become the settings on the potentiometers scaling the various terms in the equation, as indicated in Figure 13. The calculated rate of yaw is compared with the actual helicopter angular rate by introducing it into the comparator with a resistance given by

$$R_{IN_MODEL} = \frac{K_r}{K_{r_H}} \times R_{IN_HELICOPTER}$$

where $R_{IN_HELICOPTER}$ and K_{r_H} , the yaw rate gyro scaling ($\text{volts}/\frac{\text{rad}}{\text{sec}}$), remain

invariant. Similarly, as the model output scaling is altered, the lead or pre-emphasis scaling must be changed inversely to maintain proper overall operation.

Figure 13 indicates how the equation is "patched" on the computer. In any given program the parameters that are to be varied are wired into the gain setting potentiometers mounted in the cockpit, so that the safety pilot can alter them without leaving his seat.

| CHANNEL | | UNDAMPED NATURAL FREQUENCY, ω_N IN RAD/SEC | |
|---------|-------------|--|---------------------------------------|
| | | DETERMINED FROM GRAPHICAL ANALYSIS | DETERMINED FROM ACTUAL FLIGHT TEST |
| YAW | HOVER | 40.5 | 31.8 |
| | 50 KNOTS | | 30 |
| PITCH | HOVER | 9.2 | 9.5 |
| | 50 KNOTS | 10 | 12 |
| ROLL | HOVER | 10.5 | 13 |
| | 50 KNOTS | 11.1 | 11.2 |
| HEAVE | HOVER | 46 | 21 |
| | 50 KNOTS | 45 | 28 |

TABLE I
UNDAMPED NATURAL FREQUENCY FOR FOUR CONTROL LOOPS

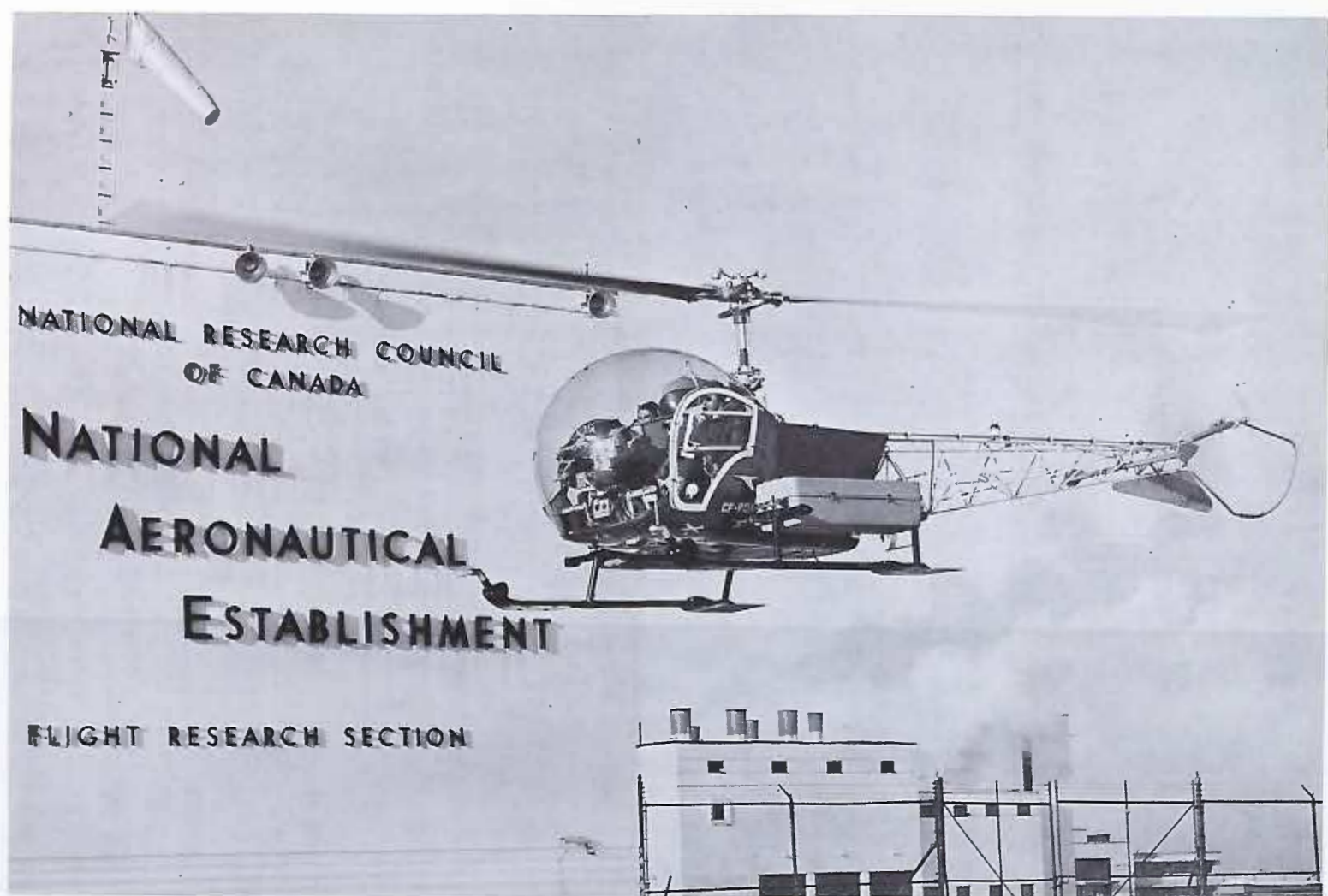


FIG. 1

FOUR DEGREES OF FREEDOM V/STOL AIRBORNE SIMULATOR

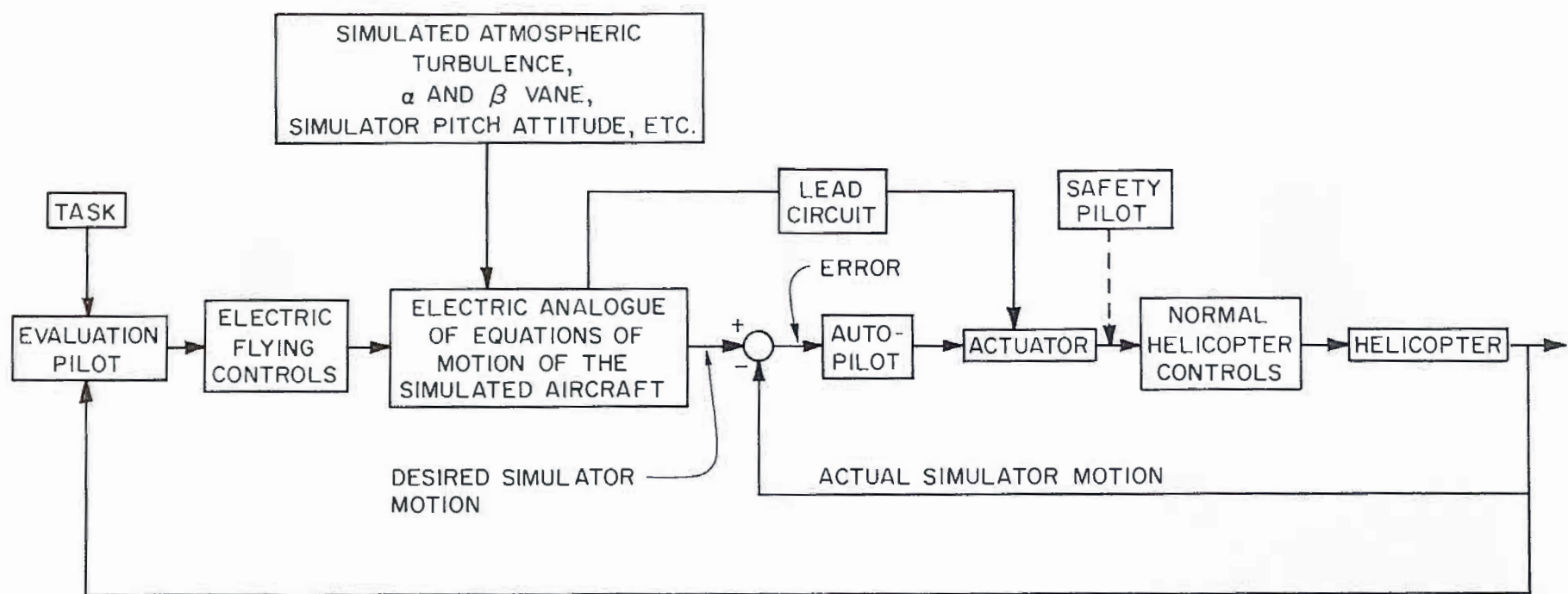


FIG. 2

"MODEL-CONTROLLED" SIMULATION METHOD

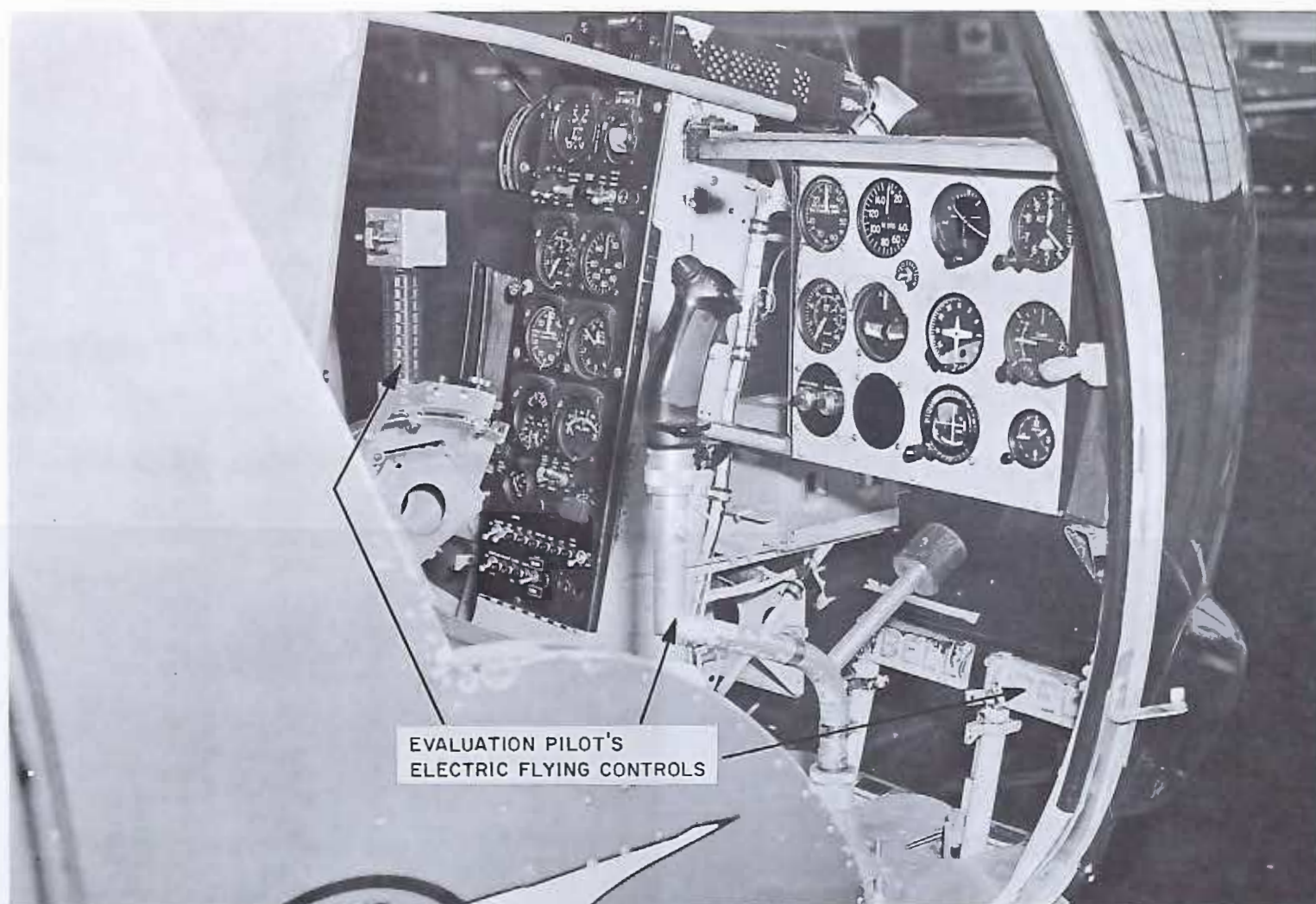


FIG. 3

VIEW OF THE SIMULATOR COCKPIT FROM THE RIGHT SIDE

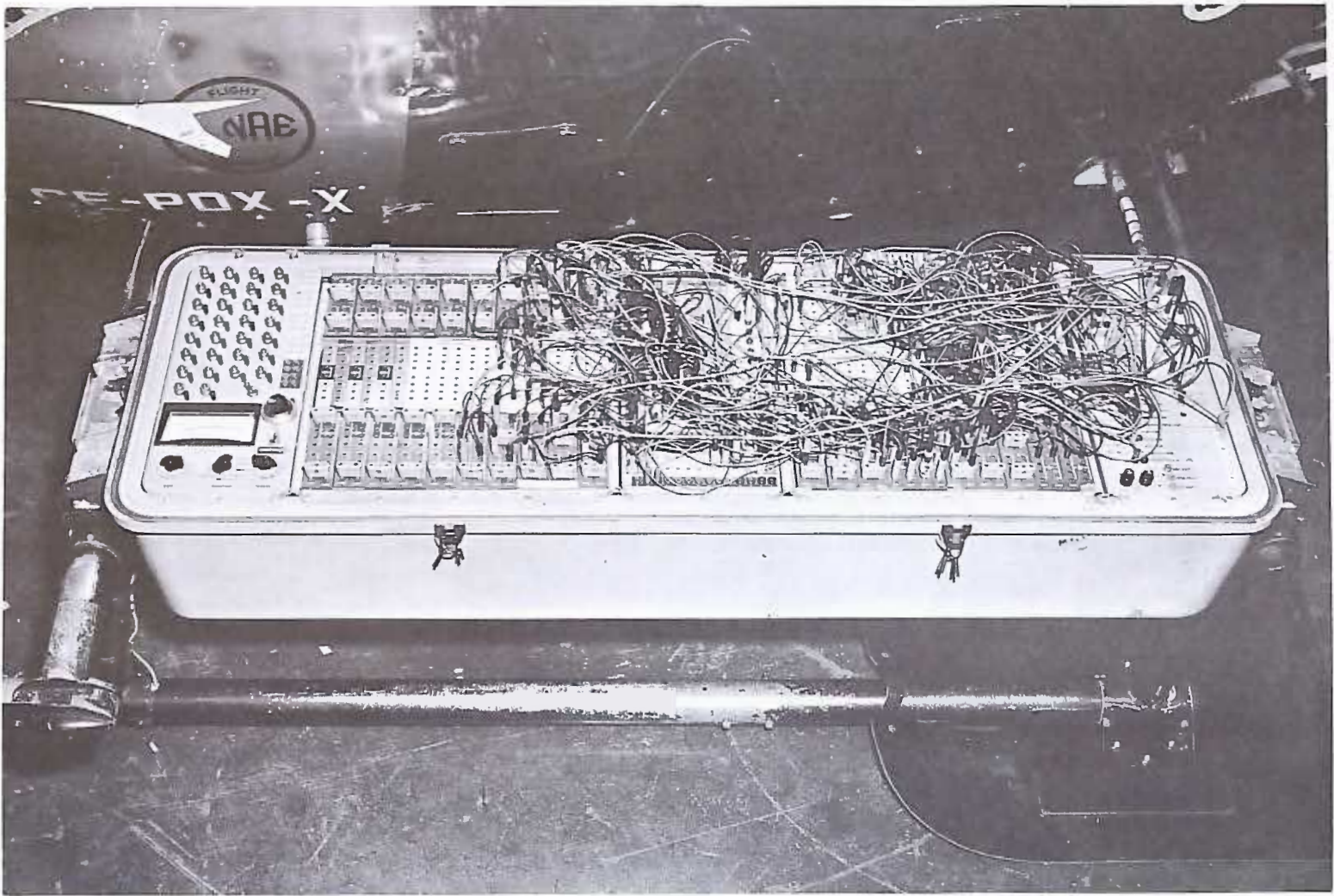


FIG. 4

THE ANALOGUE COMPUTER USED FOR THE MODEL



FIG. 5

VIEW OF THE SIMULATOR COCKPIT FROM THE LEFT SIDE

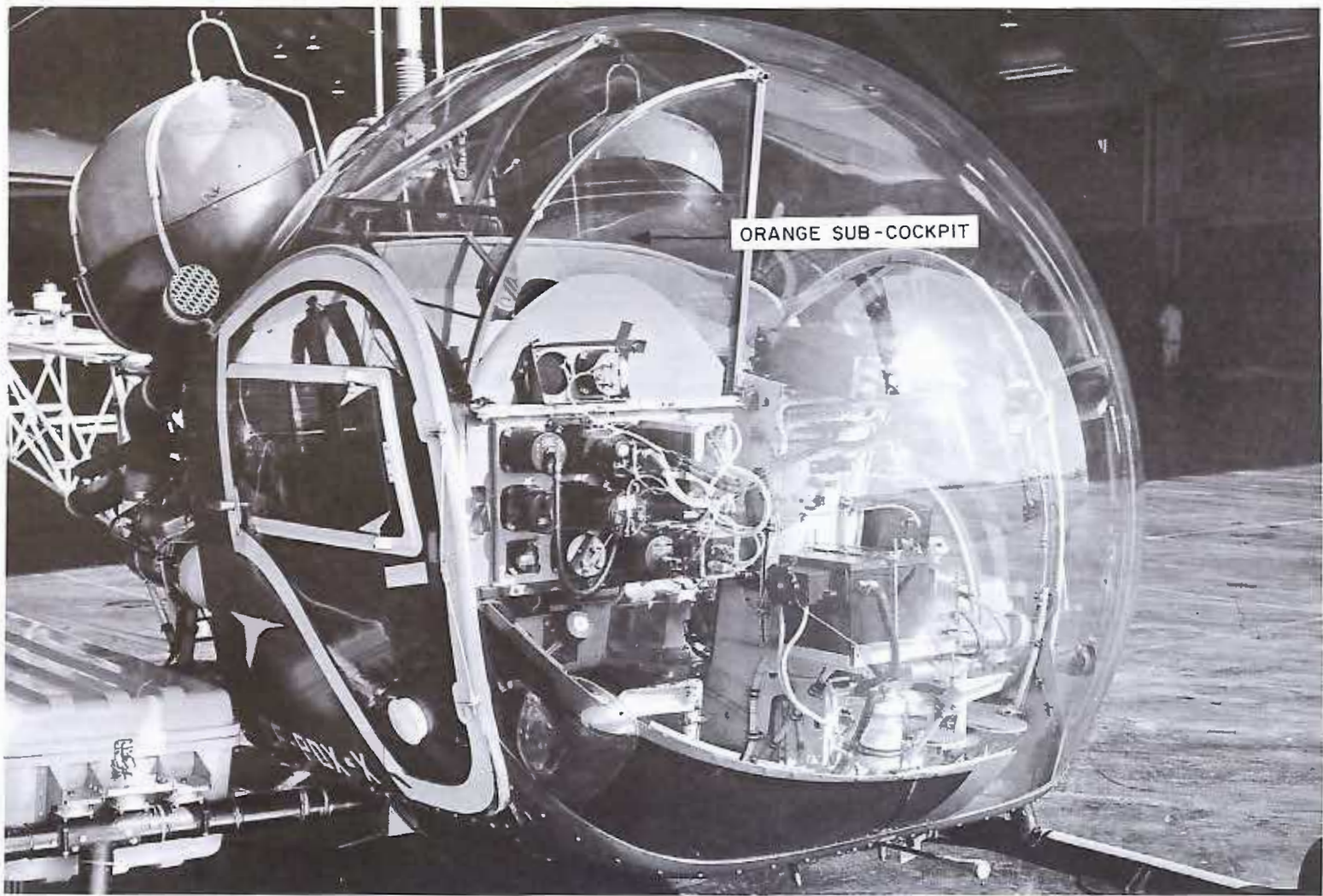


FIG. 6 ORANGE SUB-COCKPIT INSTALLATION FOR SIMULATED INSTRUMENT FLYING

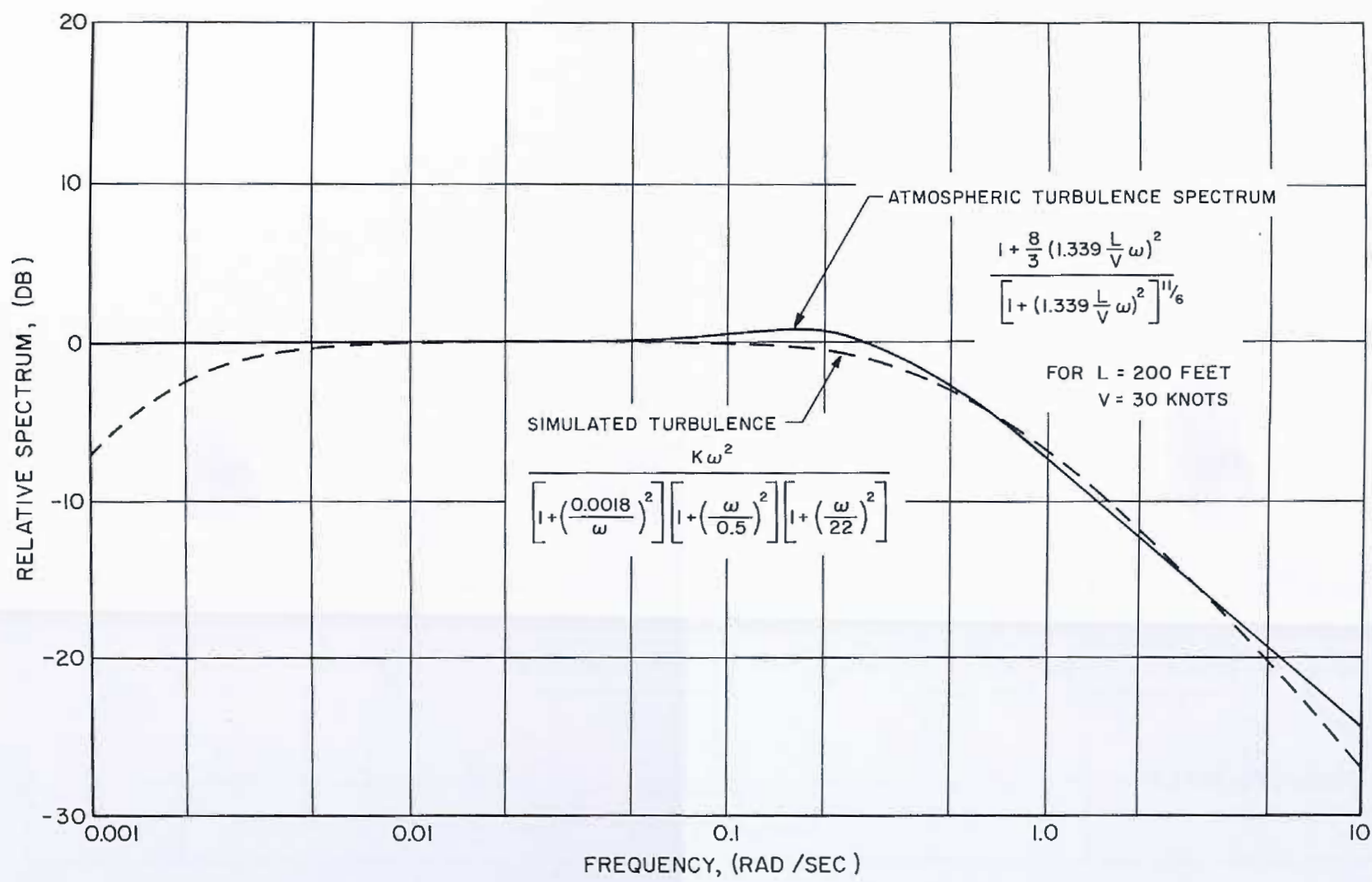


FIG. 7 POWER SPECTRUM OF SIMULATED ATMOSPHERIC TURBULENCE

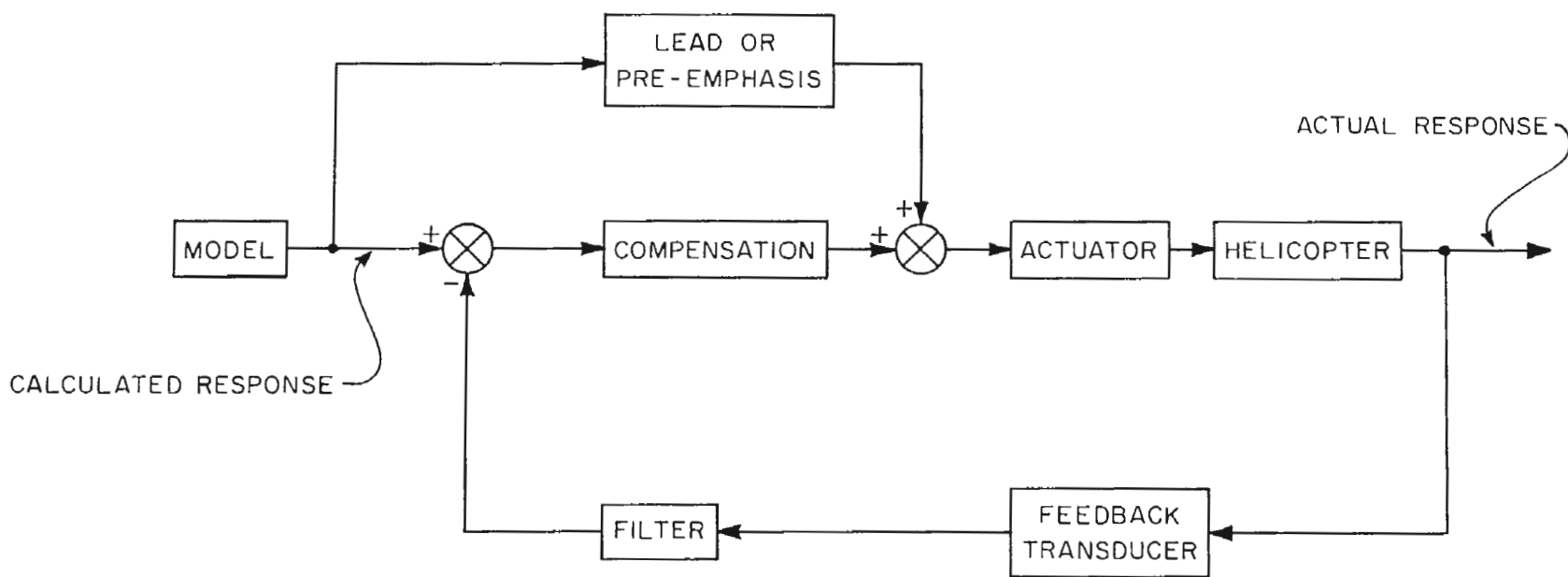


FIG. 8 AUTOPILOT SCHEMATIC

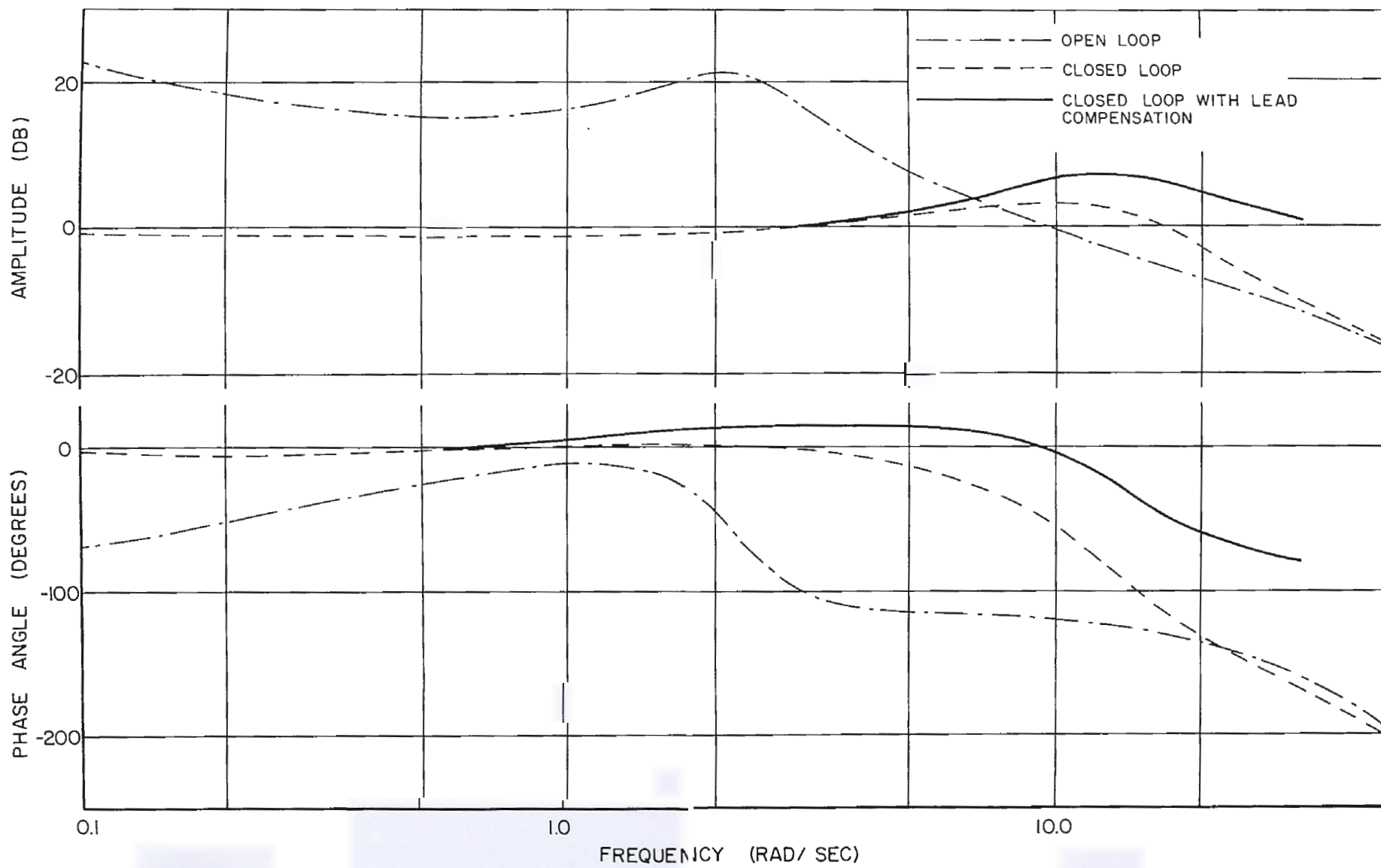


FIG. 9a FREQUENCY RESPONSE FOR YAW CONTROL LOOP

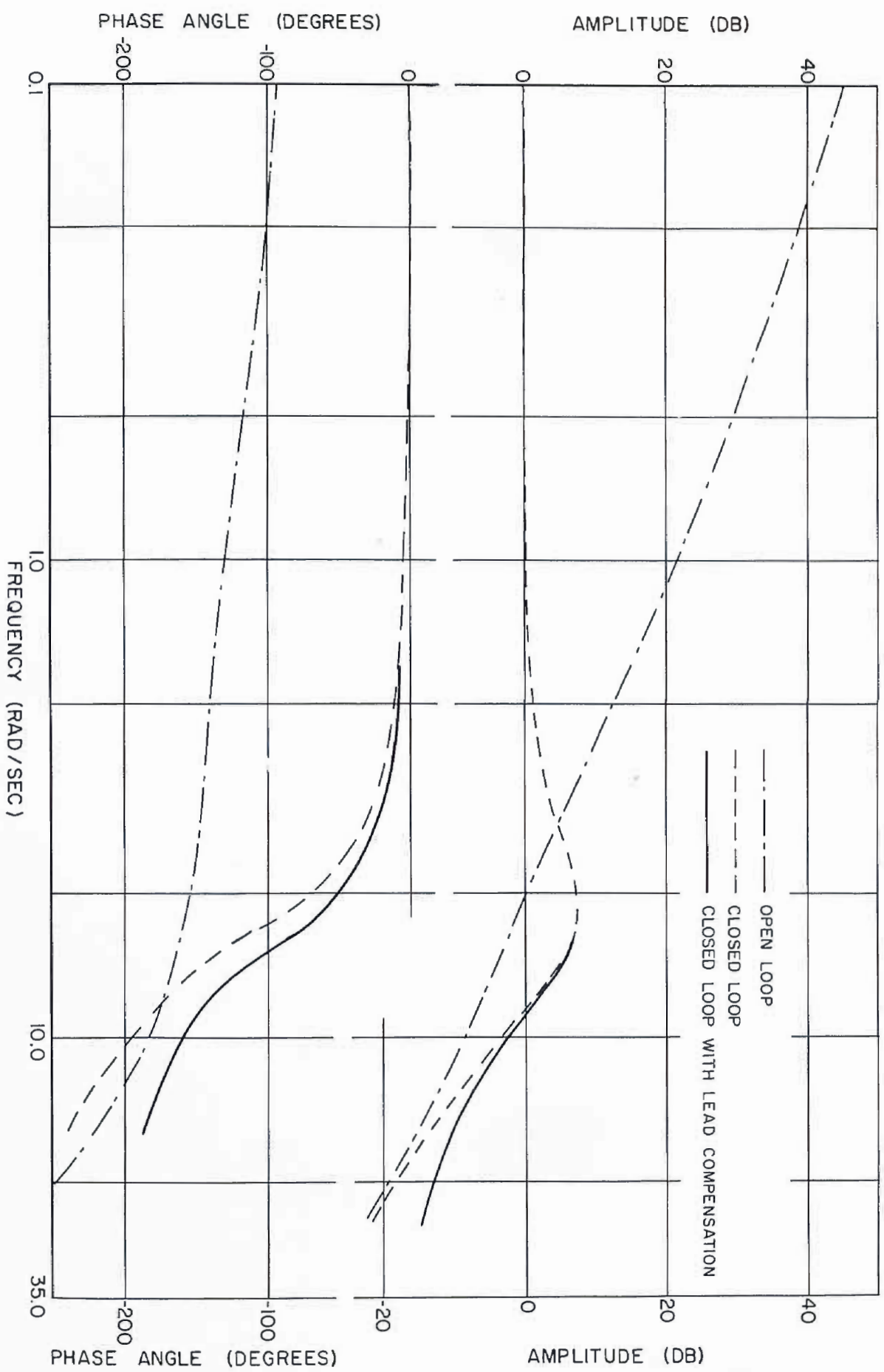


FIG. 9b

FREQUENCY RESPONSE FOR PITCH CONTROL LOOP

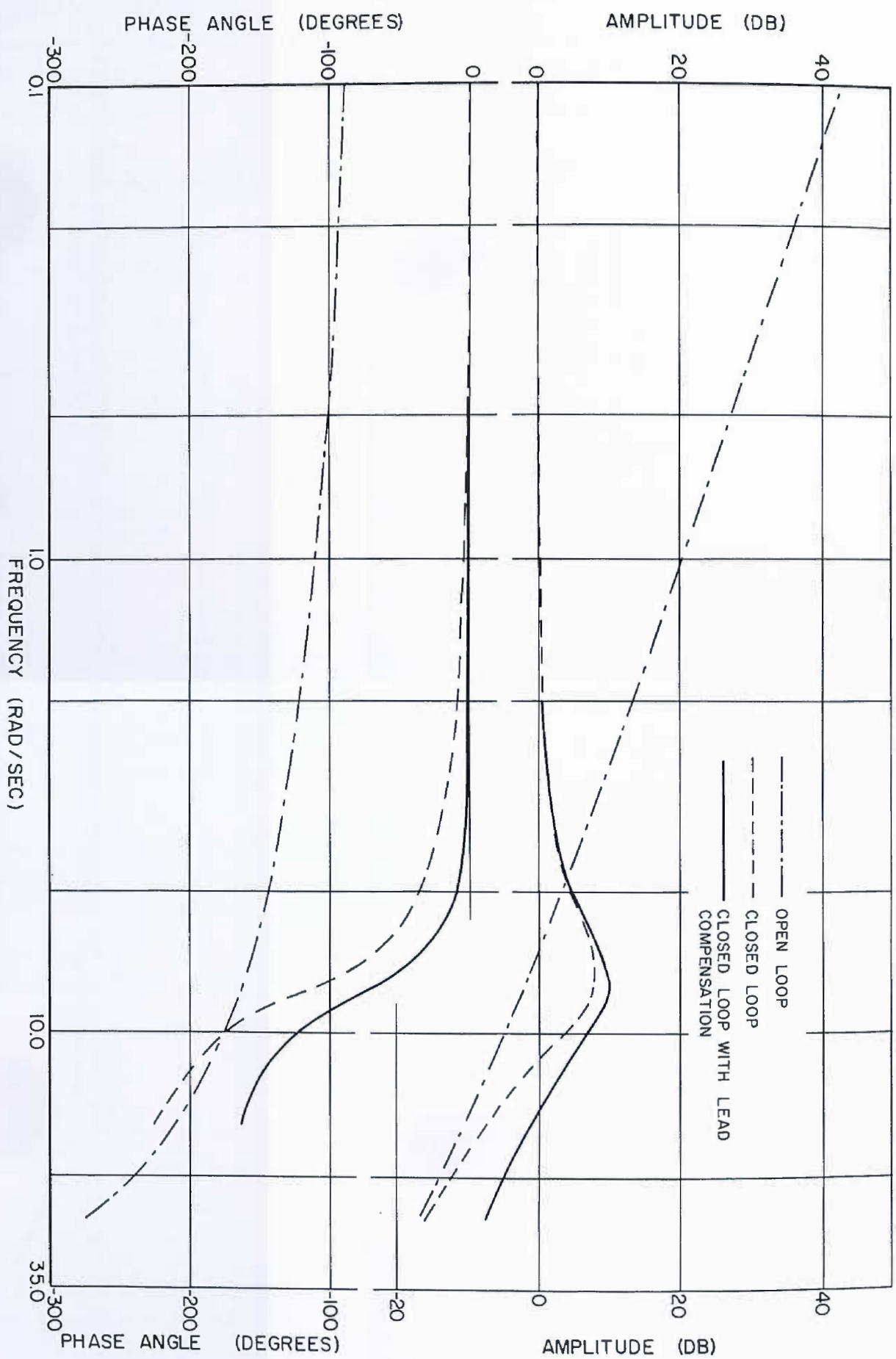


FIG. 9c

FREQUENCY RESPONSE FOR ROLL CONTROL LOOP

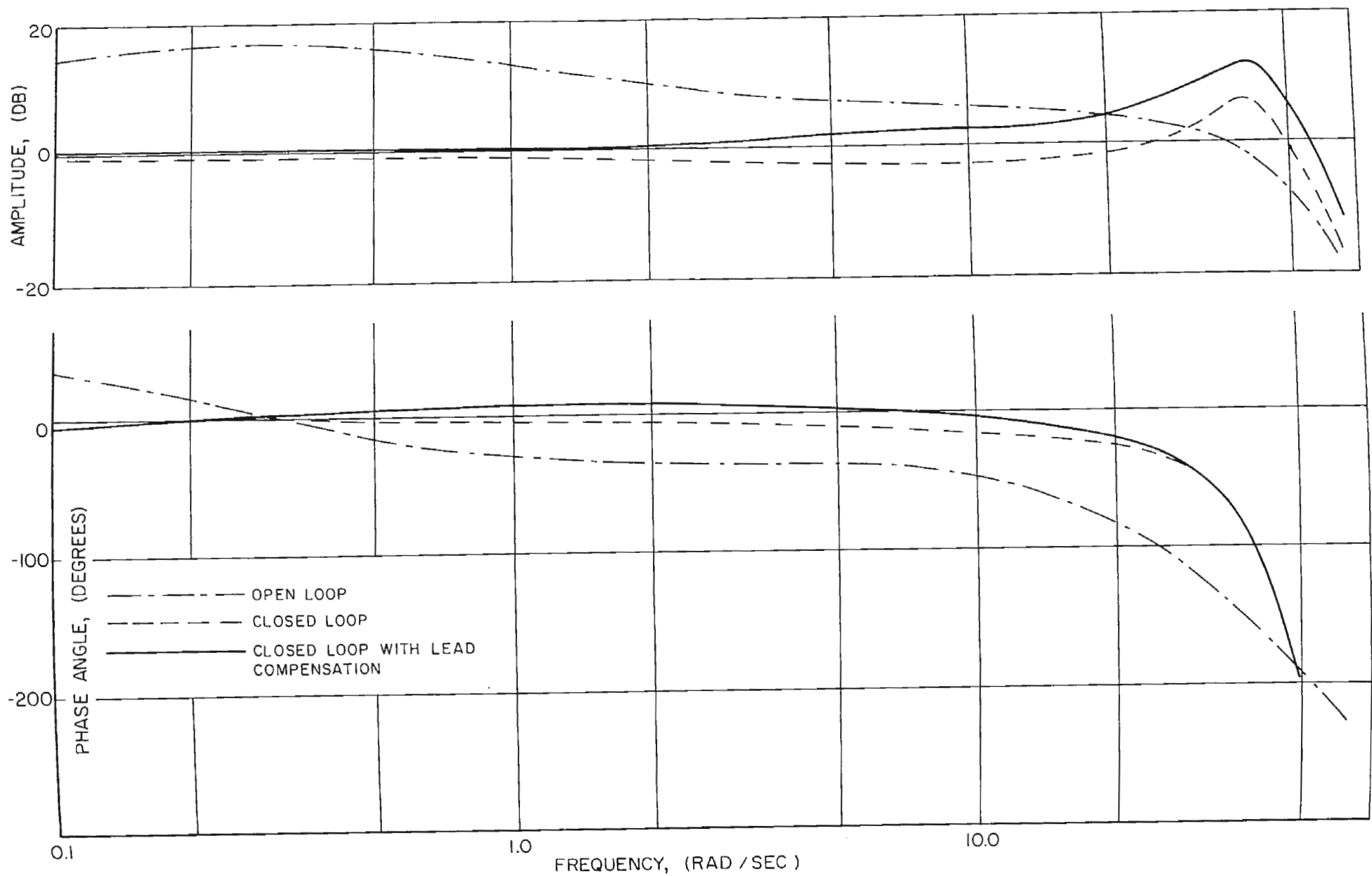


FIG. 9d

FREQUENCY RESPONSE FOR HEAVE CONTROL LOOP

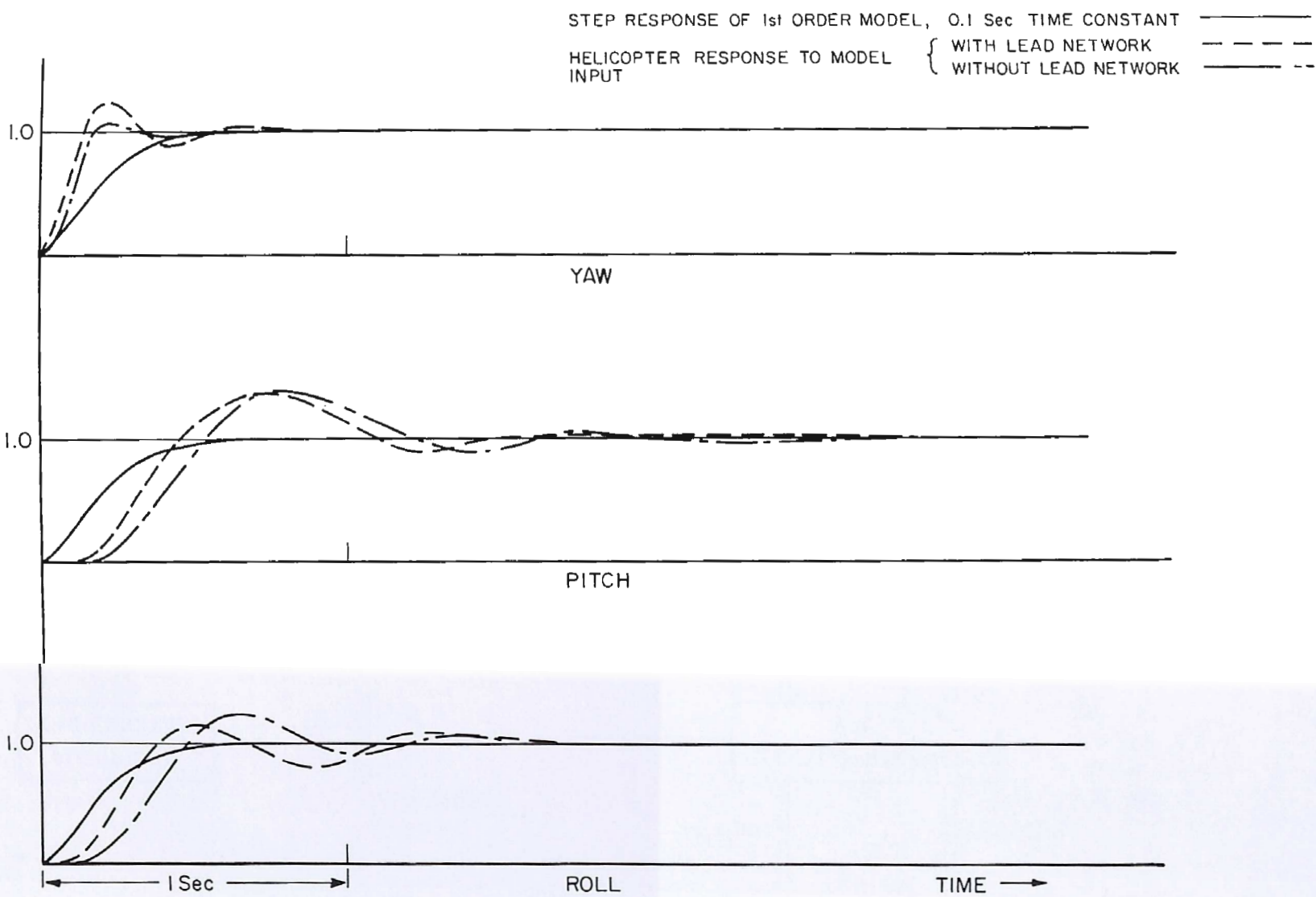


FIG. 10 ANALOGUE COMPUTER STUDY ON THE EFFECT OF LEAD NETWORK ON HELICOPTER TRANSIENT RESPONSE

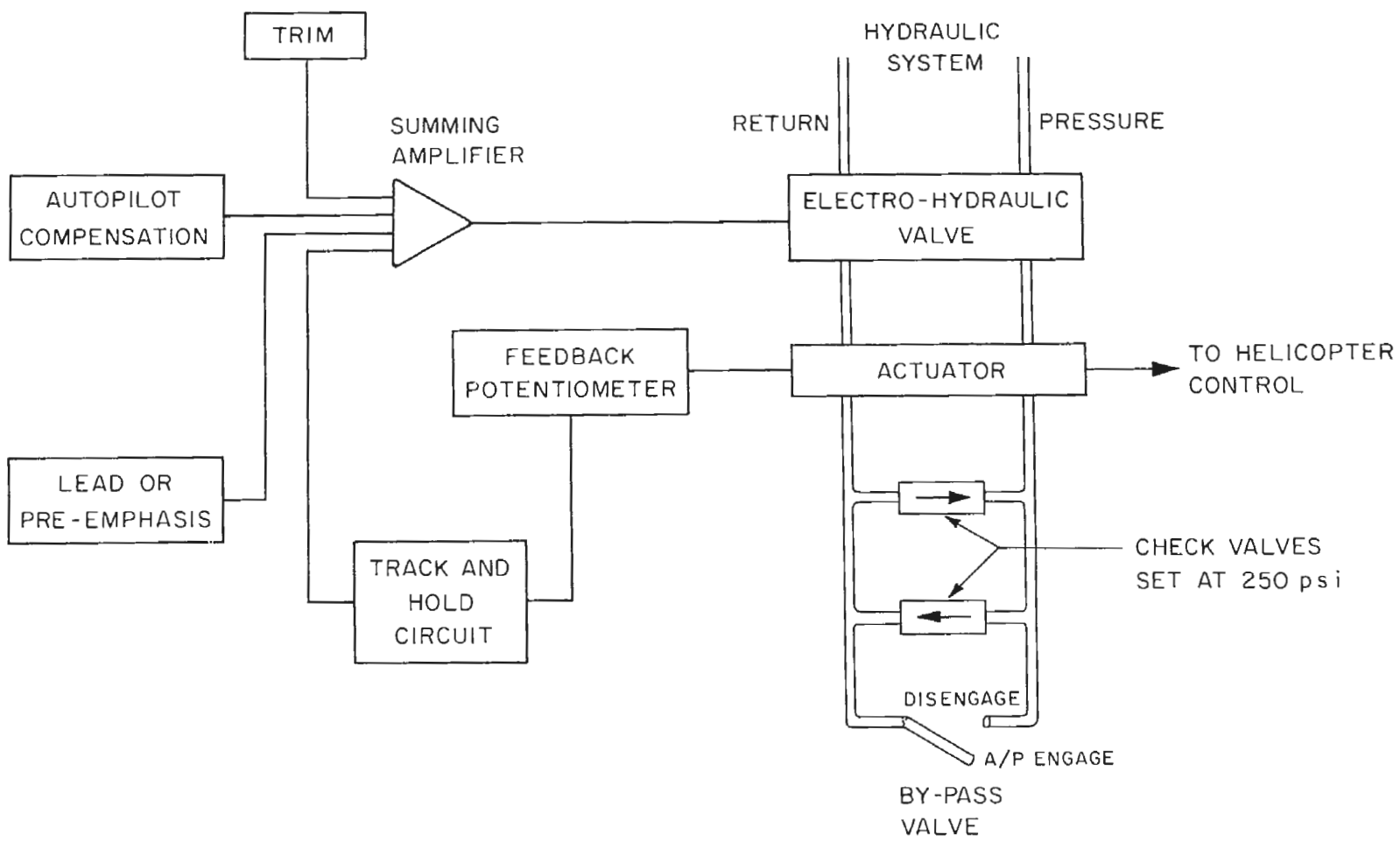


FIG. 11

AUTOPILOT ACTUATOR SYSTEM

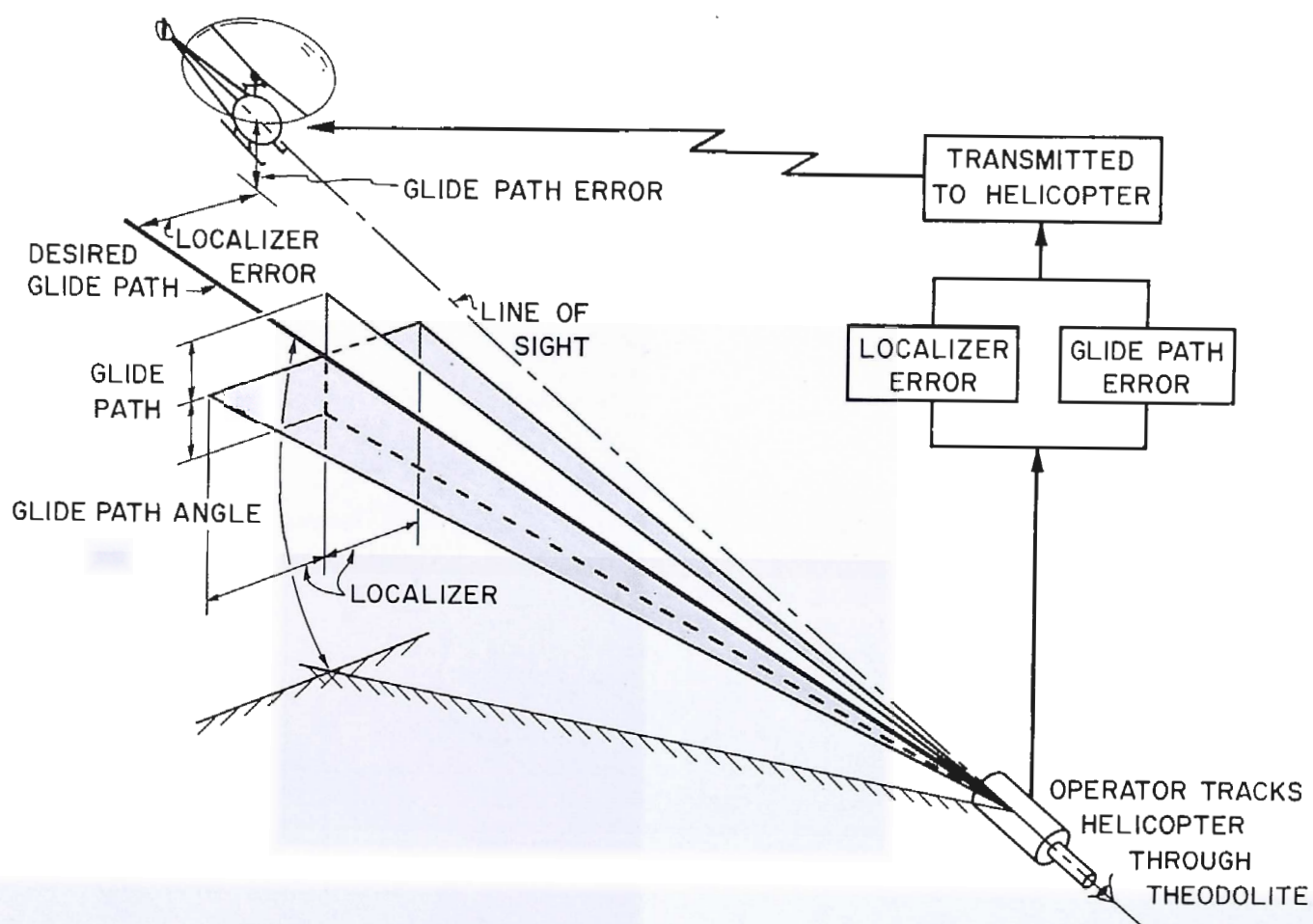


FIG. 12

SYNTHETIC INSTRUMENT LANDING SYSTEM

